

An optimization-based reformulation of the classical displacement approach for state update of non-linear material models

Z. Lotfian^a, M. V. Sivaselvan^{a,*}

^a*Department of Civil, Structural and Environmental Engineering, University at Buffalo, 212 Ketter Hall, Buffalo, NY 14260, U.S.A.*

Abstract

In this paper, we build on recent work using a mathematical programming approach for incremental state update in analysis of non-linear mechanics models. In particular, we consider quasi-static analysis of continuum problems in the linearized kinematics regime, with non-linear material models described using *convex* energy functions. We find in this case that the classical displacement-based nested approach for incremental state update can be reformulated as solving a reduced *dual* optimization problem. This reformulation provides insights into the working of the algorithm, and eliminates the need for some heuristics. An important purpose of this paper is to further illustrate the unifying nature of the mathematical programming approach. We therefore present relationships with several of these types of algorithms recently presented in the literature for incremental state update.

Keywords: mathematical programming; convex optimization; standard material; plasticity; Lagrange dual; state update

1. Introduction

Analysis of mechanics models with complex non-linear material behavior arises in different applications such as seismic response simulation of structures.

*Corresponding author

Email addresses: zahrasad@buffalo.edu (Z. Lotfian), mvs@buffalo.edu (M. V. Sivaselvan)

In a recent paper [1], we discussed the manner in which when such material behavior is described using an energy approach [2–4], *state update* of the model in each increment of a non-linear analysis can be cast into various *mathematical programs*. Depending on the type of material model, the corresponding mathematical program could assume different forms such as convex optimization, complementarity problem etc. This mathematical programming approach represents an alternative to the classical displacement-based approach. In the latter, state update is carried out in a nested fashion with displacements computed at a global level, and stresses and other internal variables computed at a material-point level. It was also seen in [1] that models of non-linear behavior that arose historically from disparate contexts, for example the Preisach model [5, 6] and the Bouc-Wen model [7–10], could be interpreted within the mathematical programming framework.

In the present paper, we further explore the unifying nature of the mathematical programming approach. We consider quasi-static continuum problems in the linearized kinematics regime, with non-linear material behavior described by convex energy functions. In this case, we find that the classical displacement-based nested approach can be reformulated as solving a reduced *dual* optimization problem. Some differentiability results related to convex optimization problems play an important role in developing this reformulation. This reformulation in turn provides insights into the working of the algorithm by means of some geometric constructions such as Figure 4, and obviates some heuristics that are otherwise used. We envision that such insights will guide development of algorithms for more complex models, for example via successive convex programs [11–14].

A particular case of non-linear material models with convex energy functions is rate-independent plasticity models. For this case, incremental state update at the material point level is known as return mapping, and has a well-known optimization format [15]. However, the optimization structure at the global level is not commonly recognized or utilized. The purpose of this paper is two-fold — (1) to reformulate the classical displacement-based nested approach for

incremental state update as an optimization problem (for quasi-static problems with convex energy functions), and (2) identify relationships with several other algorithms recently described in the literature.

This paper is organized as follows. First in section 2, governing equations presented in [1] for single-degree-of-freedom systems with energy-based material models are extended to general spatially discretized systems. With some restrictions, when discretized in time, these equations lead to an optimization problem in each time increments. In section 3, three forms of this optimization problem are discussed — a primal problem, a dual problem, and a reduced dual problem. The reduced dual problem is a reformulation of the classical displacement-based nested approach, and consists of solving an optimization sub-problem at the integration point level. Solution of the reduced dual problem is the subject of section 4. Differentiability of the objective function is considered and derivatives are obtained, so that Newton’s method for unconstrained minimization can be applied as described in section 4.2. In section 5, some special classes of material models are discussed, where the integration point level optimization problem admits a simpler solution process. A numerical example is presented in section 6 to illustrate the working of the algorithm of section 4.2. Lastly in section 7, relationships between various solution strategies presented in recent years based on the mathematical programming approach are discussed.

2. Governing equations and time discretization

We begin by formulating the governing equations for a continuum model that has been spatially discretized, for example by the finite element method. We employ a class of non-linear material models described completely by certain energy functions. As discussed in [1], such a representation of material models is based on the *generalized standard material* framework [2, 16], and is also closely related to the hyperplasticity framework [3, 17]. In this energy framework, a material model is characterized by two convex (possibly nonsmooth) functions — a stored energy function $\psi(\epsilon, \alpha)$, and a dissipation function $\phi(\dot{\epsilon}, \dot{\alpha})$, where ϵ is

the strain, and α is a vector of kinematic internal state variables (such as equivalent plastic strain, damage etc.). We refer to the Fenchel-Legendre transforms of these functions as the complementary stored energy function $\psi^c(\sigma, \zeta)$, and the complementary dissipation function $\phi^c(\sigma, \zeta)$, where σ is the stress and the ζ is the generalized stress conjugate to α . The governing equations discussed in [1] for simple single-degree-of-freedom dynamic models can be generalized to spatially discretized continuum models as

$$\begin{aligned}
\text{momentum conservation : } & \underbrace{\frac{d}{dt} \nabla \left(\frac{1}{2} \dot{v}^\top M \dot{v} \right)}_{\text{inertia force}} + \underbrace{\nabla \left(\frac{1}{2} \dot{v}^\top C_d \dot{v} \right)}_{\text{damping force}} + \underbrace{B^\top \sigma}_{\text{element force}} = p \\
\text{deformation compatibility : } & \underbrace{\frac{d}{dt} \partial_1 \psi^c(\sigma, \zeta)}_{\text{elastic deformation rate}} + \underbrace{\partial_1 \phi^c(\sigma, \zeta)}_{\text{plastic deformation rate}} - \underbrace{B v}_{\text{total deformation rate}} \ni 0 \\
\text{internal variable evolution : } & \underbrace{\frac{d}{dt} \partial_2 \psi^c(\sigma, \zeta)}_{\substack{\text{reversible internal} \\ \text{variable rate}}} + \underbrace{\partial_2 \phi^c(\sigma, \zeta)}_{\substack{\text{irreversible} \\ \text{internal variable} \\ \text{rate}}} \ni 0
\end{aligned} \tag{1}$$

Here, $v \in \mathbb{R}^{N_{\text{DOF}}}$ is the vector of free velocity components, $M, C_d \in \mathbb{R}^{N_{\text{DOF}} \times N_{\text{DOF}}}$ are respectively positive semi-definite mass and damping matrices, and $p \in \mathbb{R}^{N_{\text{DOF}}}$ is the external load vector. $\sigma \in \mathbb{R}^{N_\sigma N_G}$ is the stress vector comprised of N_σ components at each of the N_G material points. Similarly, $\zeta \in \mathbb{R}^{N_\zeta N_G}$ is the vector of generalized stress internal variable. $\psi^c, \phi^c : \mathbb{R}^{N_\sigma N_G} \times \mathbb{R}^{N_\zeta N_G} \rightarrow \mathbb{R}$ are the complementary stored energy and complementary dissipation functions. $B \in \mathbb{R}^{N_\sigma N_G \times N_{\text{DOF}}}$ is the linearized deformation-displacement matrix. ∇ denotes the gradient, and ∂ denotes the subdifferential of a nonsmooth convex function [18]. ∇_q and ∂_q denote gradient and subdifferential with respect to argument q of the function. Equations (1)_{2,3} are inclusions because ψ^c and ϕ^c could be nonsmooth, and hence have set-valued derivatives. We make the following remarks on equation (1).

1. As suggested by their format, equations (1) can be obtained as Euler-Lagrange equations of a generalized Hamilton's principle [1, 19].
2. The terminology we have used above in reference to spatial discretization follows the common setting, where displacements and velocities are asso-

ciated with nodes, and stresses and other internal variables with element integration points. However, the formulation itself is not restricted to this type of spatial discretization. For example, in a stress-based finite element, σ would denote components of the stress approximation rather than the integration point values, or in an assumed-strain finite element, v would include components of the element-level assumed strain coefficients.

3. For notational convenience, we take that equations (1)_{2,3} have been multiplied through by the appropriate integration weights and element Jacobian determinants. This explains our use of the term “deformation rate” instead of “strain rate” in equations (1)_{2,3}, and the reason why the element nodal forces can be written simply as $B^\top \sigma$ in equation (1)₁. Later in section 4.1, the tangent stiffness matrix is of the form $B^\top \square B$.
4. In the above, we consider a restricted class of material models for which ψ and ϕ are convex. One source of non-convexity is so-called *non-associated flow* in plasticity models. It can be shown that in some instances of non-associated flow models, the complementary dissipation function can be written as $\phi^c(\sigma, \zeta; \alpha)$ with explicit dependence on the kinematic internal variables [20]. Equations (1) then still apply, as discussed for simple single-degree-of-freedom systems in [1]. Explicit dependence on α then suggests solving the incremental state update as a succession of convex subproblems, computing α in an outer stage.
5. When nonlinear kinematics is considered, the term B in equations (1)_{1,2} is replaced by $D\mathcal{E}(u)$. \mathcal{E} is the nonlinear deformation-displacement map (i.e., the function that maps node displacements to element strains), u is the vector of free displacement components, and D is the derivative operator. Thus $B = D\mathcal{E}(0)$. In some instances, the kinetic energy in the first term of equation (1)₁ may also be of the form $\frac{1}{2}v^\top M(u)v$. This again suggests a successive convex programming approach, updating u in an outer stage.

For the sake of concreteness, in what follows, we introduce the following additional restrictions.

1. The complementary stored energy function ψ^c is smooth. Nonsmooth stored energy functions, such as those resulting from approximating tension- or compression-only behavior and some forms of damage, can however be treated in a similar manner to nonsmooth dissipation functions as described below [1].
2. The complementary dissipation function is of the form

$$\phi^c(\sigma, \zeta) = \sqcup_{\mathcal{C}}(\sigma, \zeta) \quad (2a)$$

where \mathcal{C} is a convex set given by

$$\mathcal{C} = \{(\sigma, \zeta) | \varphi(\sigma, \zeta) \leq 0\} \quad (2b)$$

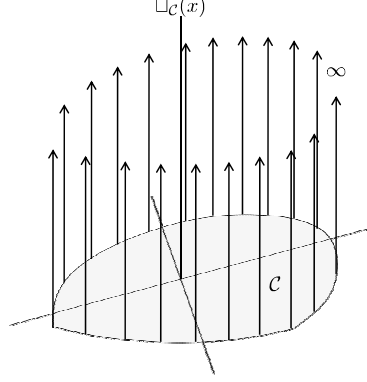
$\sqcup_{\mathcal{C}}$ is its indicator function [18] (Figure , and φ is a smooth vector-valued function, each component of which is convex. In plasticity models, φ is the yield function, and \mathcal{C} is the elastic region.

We note that this restricted framework is sufficient to describe nonlinear elastoplasticity. We assume for simplicity of presentation that there is an identical number N_y of yield functions at each material point. Thus $\varphi : \mathbb{R}^{N_\sigma N_G} \times \mathbb{R}^{N_\zeta N_G} \rightarrow \mathbb{R}^{N_y N_G}$. With the restriction (2), the subdifferential of ϕ^c that appears in equations (1)_{2,3} can be written as (Figure 1b)

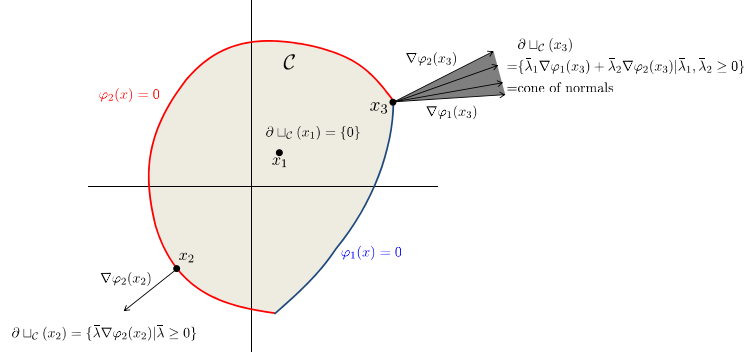
$$\partial\phi^c(\sigma, \zeta) = \{\bar{\lambda}^\top \nabla \varphi(\sigma, \zeta) | \varphi(\sigma, \zeta) \leq 0, \bar{\lambda} \geq 0, \bar{\lambda}^\top \varphi(\sigma, \zeta) = 0\} \quad (3)$$

For quasi-static analyses, the first two terms of equation (1)₁ are absent. Also using the fact that ψ^c has been restricted to being smooth and equation (3), equations (1) can be written in the alternate form

$$\begin{aligned} B^\top \sigma &= p \\ \frac{d}{dt} \nabla_1 \psi^c(\sigma, \zeta) + \bar{\lambda}^\top \nabla_1 \varphi(\sigma, \zeta) - Bv &= 0 \\ \frac{d}{dt} \nabla_2 \psi^c(\sigma, \zeta) + \bar{\lambda}^\top \nabla_2 \varphi(\sigma, \zeta) &= 0 \\ \varphi(\sigma, \zeta) &\geq 0, \quad \bar{\lambda} \geq 0, \quad \bar{\lambda}^\top \varphi(\sigma, \zeta) = 0 \end{aligned} \quad (4)$$



(a) Indicator function of a convex subset \mathcal{C} of \mathbb{R}^2



(b) Subdifferential of the indicator function of \mathcal{C} ; The subdifferential is shown at three points — x_1 in the interior if \mathcal{C} , x_2 where the boundary is smooth, and x_3 where the boundary is not smooth

Figure 1: Indicator function and its subdifferential for a convex set $\mathcal{C} = \{x \in \mathbb{R}^n \mid \varphi_i(x) \leq 0, i = 1, 2\}$

Equations (4) may be formally discretized in time. Using Backward Euler with a time increment Δt , we get

$$\begin{aligned}
 B^\top \sigma^{n+1} &= p^{n+1} \\
 \frac{\nabla_1 \psi^c(\sigma^{n+1}, \zeta^{n+1}) - \nabla_1 \psi^c(\sigma^n, \zeta^n)}{\Delta t} + (\bar{\lambda}^{n+1})^\top \nabla_1 \varphi(\sigma^{n+1}, \zeta^{n+1}) - B \frac{u^{n+1} - u^n}{\Delta t} &= 0 \\
 \frac{\nabla_2 \psi^c(\sigma^{n+1}, \zeta^{n+1}) - \nabla_2 \psi^c(\sigma^n, \zeta^n)}{\Delta t} + (\bar{\lambda}^{n+1})^\top \nabla_2 \varphi(\sigma^{n+1}, \zeta^{n+1}) &= 0 \\
 \varphi(\sigma^{n+1}, \zeta^{n+1}) \geq 0, \quad \bar{\lambda}^{n+1} \geq 0, \quad (\bar{\lambda}^{n+1})^\top \varphi(\sigma^{n+1}, \zeta^{n+1}) &= 0
 \end{aligned} \tag{5}$$

where $u \in \mathbb{R}^{N_{\text{DOF}}}$ is the vector of free displacements. Multiplying equations (5)_{2,3} by Δt , rearranging, and introducing the symbols $\mu := u^{n+1} - u^n$ and $\lambda := \Delta t \bar{\lambda}$, equations (5) become

$$\begin{aligned} \nabla_1 \psi^c(\sigma^{n+1}, \zeta^{n+1}) + \lambda^\top \nabla_1 \varphi(\sigma^{n+1}, \zeta^{n+1}) - (B\mu + \underbrace{\nabla_1 \psi^c(\sigma^n, \zeta^n)}_{=: b_\sigma}) &= 0 \\ \nabla_2 \psi^c(\sigma^{n+1}, \zeta^{n+1}) + \lambda^\top \nabla_2 \varphi(\sigma^{n+1}, \zeta^{n+1}) - \underbrace{\nabla_2 \psi^c(\sigma^n, \zeta^n)}_{=: b_\zeta} &= 0 \end{aligned} \quad (6)$$

$$B^\top \sigma^{n+1} = p^{n+1}$$

$$\varphi(\sigma^{n+1}, \zeta^{n+1}) \geq 0, \quad \lambda \geq 0, \quad \lambda^\top \varphi(\sigma^{n+1}, \zeta^{n+1}) = 0$$

Equations (6) become the starting point for optimization problems of different forms as discussed in the next section. We note that prescribed displacements can be accounted for by simply replacing all occurrences of the term $(B\mu + b_\sigma)$ above by $(B\mu + B^{\text{prsc}}\mu^{\text{prsc}} + b_\sigma)$, where μ^{prsc} is the increment of prescribed displacements, and B^{prsc} is the deformation-displacement displacement matrix associated with DOF with prescribed displacement.

3. Optimization problems

3.1. Primal optimization problem

We recognize immediately that equations (6) are the Karush-Kuhn-Tucker optimality (KKT) conditions [21] for the following minimization problem.

$$\begin{aligned} (\sigma^{n+1}, \zeta^{n+1}) &= \underset{(\sigma, \zeta)}{\operatorname{argmin}} \quad \psi^c(\sigma, \zeta) - b_\sigma^\top \sigma - b_\zeta^\top \zeta \\ &\text{subject to } B^\top \sigma = p^{n+1} \\ &\quad \varphi(\sigma, \zeta) \leq 0 \end{aligned} \quad (7)$$

where b_σ and b_ζ are as defined in equation (6). The incremental displacements are the Lagrange multipliers corresponding to the equilibrium constraints (motivating the notation μ). The Lagrange multipliers λ corresponding to the yield constraints can be interpreted as incremental equivalent plastic strains.

(7) is a convex minimization problem, since the objective function and inequality constraints are convex, and the equality constraint is linear [22]. We refer to this as the *primal* optimization problem. We note that (7) corresponds to the mathematical program referred to as “approach 1” in [1]. It is identical to equation (46) of reference [23] (where the notation κ is used for ζ), and similar to equation (5) in [24]. It is also the same as equation (17) in [25], where dynamics is considered as well (and the notation (F, ζ) is used for (σ, ζ)). We assume in the following that

1. (7) has a solution.
2. ψ^c is strongly convex, so that the solution of (7) is unique, and the min in equation (11) is meaningful.
3. (7) satisfies Slater’s constraint qualification condition [22], i.e. that it has a strictly feasible point.

We write (7) in a more convenient form by noting that the objective function and the constraints are *separable* over integrations points. The objective function can be written as

$$\Pi^c(\sigma, \zeta) := \sum_{m=1}^{N_G} \psi^c(\sigma_m, \zeta_m) - b_{\sigma m}^\top \sigma_m - b_{\zeta m}^\top \zeta_m \quad (8)$$

and the optimization problem as

$$\begin{aligned} (\sigma^{n+1}, \zeta^{n+1}) &= \underset{(\sigma, \zeta)}{\operatorname{argmin}} \Pi^c(\sigma, \zeta) \\ \text{subject to } &\sum_{m=1}^{N_G} B_m^\top \sigma_m = p \\ &\varphi(\sigma_m, \zeta_m) \leq 0, \quad m = 1, \dots, N_G \end{aligned} \quad (\text{PRIMAL})$$

where subscript m denotes components of a vector or rows of a matrix corresponding to integration point m . We have used ψ^c and φ in the above equations instead of ψ_m^c and φ_m , to minimize notational clutter. Models where the material is not homogenous, so that these functions are different at different integration points presents no additional difficulty. We have also dropped the superscript $n + 1$ on the load vector p for brevity.

The Lagrangian associated with (PRIMAL) is

$$\begin{aligned}
\mathcal{L}\left(\begin{pmatrix} \sigma \\ \zeta \end{pmatrix}, \begin{pmatrix} \mu \\ \lambda \end{pmatrix}\right) &= \Pi^c(\sigma, \zeta) - \mu^\top \left(\sum_{m=1}^{N_G} B_m^\top \sigma_m - p \right) + \sum_{m=1}^{N_G} \lambda_m^\top \varphi(\sigma_m, \zeta_m) \\
&= \mu^\top p + \sum_{m=1}^{N_G} [\psi^c(\sigma_m, \zeta_m) + \lambda_m^\top \varphi(\sigma_m, \zeta_m) - (B_m \mu + b_{\sigma m})^\top \sigma_m - b_{\zeta m}^\top \zeta_m] \\
&= \mu^\top p + \sum_{m=1}^{N_G} \mathcal{L}_m\left(\begin{pmatrix} \sigma_m \\ \zeta_m \end{pmatrix}, \begin{pmatrix} \mu \\ \lambda_m \end{pmatrix}\right)
\end{aligned} \tag{9}$$

where we have defined

$$\mathcal{L}_m\left(\begin{pmatrix} \sigma_m \\ \zeta_m \end{pmatrix}, \begin{pmatrix} \mu \\ \lambda_m \end{pmatrix}\right) := \psi^c(\sigma_m, \zeta_m) + \lambda_m^\top \varphi(\sigma_m, \zeta_m) - (B_m \mu + b_{\sigma m})^\top \sigma_m - b_{\zeta m}^\top \zeta_m \tag{10}$$

The Karush-Kuhn-Tucker (KKT) optimality conditions for (PRIMAL) follow from the Lagrangian (9) as

$$\begin{aligned}
\frac{\partial \mathcal{L}}{\partial \sigma_m} = 0 : D_1 \psi^c(\sigma_m, \zeta_m) + \lambda_m^\top D_1 \varphi(\sigma_m, \zeta_m) - (B_m \mu + b_{\sigma m})^\top &= 0, \quad m = 1, \dots, N_G \\
\frac{\partial \mathcal{L}}{\partial \zeta_m} = 0 : D_2 \psi^c(\sigma_m, \zeta_m) + \lambda_m^\top D_2 \varphi(\sigma_m, \zeta_m) - b_{\zeta m}^\top &= 0, \quad m = 1, \dots, N_G \\
\sum_{m=1}^{N_G} B_m^\top \sigma_m &= p \\
\varphi(\sigma_m, \zeta_m) \leq 0, \quad \lambda_m \geq 0, \quad \lambda_m^\top \varphi(\sigma_m, \zeta_m) &= 0, \quad m = 1, \dots, N_G
\end{aligned} \tag{KKT}$$

These are merely equations (6) separated over the integration points. Since the gradient is the transpose of the derivative, while equations (6)_{1,2} are in terms of column vectors, equations (KKT)_{1,2} are in terms of row vectors. We next construct the dual of problem (PRIMAL), which in section 4 leads to a reformulation of the classical displacement-based approach as an optimization problem.

3.2. Dual optimization problem

Duality is familiar in mechanics from the classical principles of total potential energy and total complementary potential energy, and from the upper- and lower-bound theorems of limit analysis. Associated with every optimization

problem is a dual problem, which often has a useful interpretation. For convex problems such as (PRIMAL) that satisfy constraint qualification conditions as assumed above, *strong duality* holds. This means that a dual optimal solution is equal in objective function value to a primal optimal solution, and that the primal-dual solution pair satisfies the KKT conditions. The KKT conditions are also sufficient conditions for a solution of the primal problem [22].

To construct the dual problem for (PRIMAL), we start from the Lagrange dual function [22], defined as the minimum of the Lagrangian of Π^c over (σ, ζ) .

$$-\Pi(\mu, \lambda) := \min_{(\sigma, \zeta)} \mathcal{L}\left(\begin{pmatrix} \sigma \\ \zeta \end{pmatrix}, \begin{pmatrix} \mu \\ \lambda \end{pmatrix}\right) \quad (11)$$

We are able to write min here instead of inf, because of the strong convexity assumption on ψ^c . Let $(\sigma_m^*, \zeta_m^*), m = 1, \dots, N_G$ be the minimizers in (11). Functions $\sigma_m^*(\mu, \lambda)$ and $\zeta_m^*(\mu, \lambda)$ are then implicitly defined by the following optimality conditions.

$$\begin{aligned} D_1 \psi^c(\sigma_m^*(\mu, \lambda), \zeta_m^*(\mu, \lambda)) + \lambda_m^\top D_1 \varphi(\sigma_m^*(\mu, \lambda), \zeta_m^*(\mu, \lambda)) - (B_m \mu + b_{\sigma m})^\top &= 0 \\ D_2 \psi^c(\sigma_m^*(\mu, \lambda), \zeta_m^*(\mu, \lambda)) + \lambda_m^\top D_2 \varphi(\sigma_m^*(\mu, \lambda), \zeta_m^*(\mu, \lambda)) - b_{\zeta m}^\top &= 0 \end{aligned} \quad (12)$$

i.e., given (μ, λ) , the functions $\sigma_m^*(\mu, \lambda)$ and $\zeta_m^*(\mu, \lambda)$ can be evaluated by solving equation (12). Clearly, this is equivalent to unconstrained minimization of the Lagrangian function of equation (10).

The Lagrange dual function Π of equation (11) may be written explicitly as

$$\begin{aligned} \Pi(\mu, \lambda) = -\mu^\top p - \sum_{m=1}^{N_G} \left[\psi^c(\sigma_m^*(\mu, \lambda), \zeta_m^*(\mu, \lambda)) + \lambda_m^\top \varphi(\sigma_m^*(\mu, \lambda), \zeta_m^*(\mu, \lambda)) \right. \\ \left. - (B_m \mu + b_{\sigma m})^\top \sigma_m^*(\mu, \lambda) - b_{\zeta m}^\top \zeta_m^*(\mu, \lambda) \right] \end{aligned} \quad (13)$$

The dual optimization problem corresponding to (PRIMAL) is then

$$\begin{aligned} \min \Pi(\mu, \lambda) \\ \text{subject to } \lambda \geq 0 \end{aligned} \quad (\text{DUAL})$$

As discussed above, solving this problem is completely equivalent to solving (PRIMAL). (DUAL) is a convex optimization problem with *simple bound con-*

straints. It is closely related to the mathematical program referred to as approach 2 in [1]. In section 3.3 next, we reduce this to an unconstrained optimization problem in μ alone. This forms the basis for reformulation of the classical displacement-based approach in section 4.

3.3. Reduced dual problem

Due to the separability of the objective function Π , minimization over λ in (DUAL) may be carried into the summation in (13). Thus defining the function

$$\begin{aligned} \bar{\Pi}(\mu) := -\mu^\top p - \sum_{m=1}^{N_G} \min_{\lambda_m \geq 0} & \left[\psi^c(\sigma_m^*(\mu, \lambda), \zeta_m^*(\mu, \lambda)) + \lambda_m^\top \varphi(\sigma_m^*(\mu, \lambda), \zeta_m^*(\mu, \lambda)) \right. \\ & \left. - (B_m \mu + b_{\sigma m})^\top \sigma_m^*(\mu, \lambda) - b_{\zeta m}^\top \zeta_m^*(\mu, \lambda) \right] \end{aligned} \quad (14)$$

(DUAL) can be reduced to minimization of μ alone as

$$\min_{\mu} \bar{\Pi}(\mu) \quad (\text{REDUCED})$$

This reduced problem leads to the reformulation of classical displacement-based approach as an optimization problem. We note that in this way, the solution of (DUAL) is carried out in a nested fashion — the minimization over $\lambda_m \geq 0$ within the summation is at the integration point level, while the minimization over μ is at the global level. We reiterate that the integration point-level minimization format is well-known in the context of so-called return-mapping schemes, discussed further in section 5. However, the minimization structure at the global level (REDUCED) is not commonly recognized. We take on the solution of (REDUCED) in section 4. In the remainder of this section, we develop an explicit expression for $\bar{\Pi}$.

Consider the minimization within the summation in equation (14).

$$\begin{aligned} \min_{\lambda_m} & \psi^c(\sigma_m^*(\mu, \lambda), \zeta_m^*(\mu, \lambda)) + \lambda_m^\top \varphi(\sigma_m^*(\mu, \lambda), \zeta_m^*(\mu, \lambda)) \\ & - (B_m \mu + b_{\sigma m})^\top \sigma_m^*(\mu, \lambda) - b_{\zeta m}^\top \zeta_m^*(\mu, \lambda) \end{aligned} \quad (\text{IPDUAL})$$

subject to $\lambda_m \geq 0$

where the prefix IP is used in the equation tag since the minimization is at the integration point level. Let $\tilde{\lambda}_m(\mu)$ be the minimizer. We recognize that (IPDUAL) is the Lagrange dual of

$$\begin{aligned} \min_{\sigma, \zeta} \quad & \psi^c(\sigma, \zeta) - (B_m \mu + b_{\sigma m})^\top \sigma - b_{\zeta m}^\top \zeta \\ \text{subject to} \quad & \varphi(\sigma, \zeta) \leq 0 \end{aligned} \tag{IPPRIMAL}$$

Let $(\tilde{\sigma}_m(\mu), \tilde{\zeta}_m(\mu))$ be the minimizer, given implicitly by the optimality conditions

$$\begin{aligned} D_1 \psi^c(\tilde{\sigma}_m(\mu), \tilde{\zeta}_m(\mu)) + \tilde{\lambda}_m(\mu)^\top D_1 \varphi(\tilde{\sigma}_m(\mu), \tilde{\zeta}_m(\mu)) - (B_m \mu + b_{\sigma m})^\top &= 0 \\ D_2 \psi^c(\tilde{\sigma}_m(\mu), \tilde{\zeta}_m(\mu)) + \tilde{\lambda}_m(\mu)^\top D_2 \varphi(\tilde{\sigma}_m(\mu), \tilde{\zeta}_m(\mu)) - b_{\zeta m}^\top &= 0 \\ \varphi(\tilde{\sigma}_m(\mu), \tilde{\zeta}_m(\mu)) \leq 0, \quad \tilde{\lambda}_m(\mu) \geq 0, \quad \tilde{\lambda}_m(\mu)^\top \varphi(\tilde{\sigma}_m(\mu), \tilde{\zeta}_m(\mu)) &= 0 \end{aligned} \tag{15}$$

By strong duality, the optimum values of (IPDUAL) and (IPPRIMAL) are identical. Therefore, $\bar{\Pi}$ can be written as

$$\bar{\Pi}(\mu) = -\mu^\top p - \sum_{m=1}^{N_G} \left[\psi^c(\tilde{\sigma}_m(\mu), \tilde{\zeta}_m(\mu)) - (B_m \mu + b_{\sigma m})^\top \tilde{\sigma}_m(\mu) - b_{\zeta m}^\top \tilde{\zeta}_m(\mu) \right] \tag{16}$$

We note as an aside that $(\tilde{\sigma}_m(\mu), \tilde{\zeta}_m(\mu), \tilde{\lambda}_m(\mu))$ solve the KKT conditions of (IPPRIMAL), and that the identities $\sigma_m^*(\mu, \tilde{\lambda}_m(\mu)) = \tilde{\sigma}_m(\mu)$ and $\zeta_m^*(\mu, \tilde{\lambda}_m(\mu)) = \tilde{\zeta}_m(\mu)$ hold. Equation (16) provides an explicit expression for $\bar{\Pi}$. In the next section, we present an algorithm for its minimization, i.e. to solve (REDUCED).

4. Optimization reformulation of the classical displacement-based nested approach

In this section, we consider numerical solution of the reduced dual problem (REDUCED). We seek to use Newton's method for unconstrained optimization. For this, we require the first and second derivatives of the objective function (16). We discuss differentiability of this function, and computation of these derivatives in section 4.1 below. We then present Newton's method in section 4.2. Solving

the reduced dual problem in this manner may be interpreted as a reformulation of the classical displacement-based nested approach as an optimization problem. The reason for this interpretation is also discussed in section 4.1.

4.1. Differentiability and derivatives

We seek to obtain the first and second derivatives of $\bar{\Pi}$ needed for minimization using Newton's method. In computing these derivatives, it is helpful to think of (IPPRIMAL) as a parametric convex optimization problem with parameter μ . The first derivative of $\bar{\Pi}$ is well-defined, and can be obtained by differentiating (16) as

$$\nabla \bar{\Pi}(\mu) = \sum_{m=1}^{N_G} B_m^\top \tilde{\sigma}_m(\mu) - p \quad (17)$$

The optimality condition for (REDUCED), $\nabla \bar{\Pi}(\mu) = 0$, is thus

$$\sum_{m=1}^{N_G} B_m^\top \tilde{\sigma}_m(\mu) = p \quad (18)$$

which is the equilibrium equation.

Equation (18) can also be obtained directly from (6), since $(6)_{1,2,4}$ are the KKT conditions of (IPPRIMAL). When derived this way however, the minimization structure (REDUCED) at the global level is not obvious. Recognizing this structure enables direct application of Newton's method for unconstrained minimization in section 4.2, without need for heuristics, often used for example in step-length determination. The classical displacement-based nested approach used (18) as the starting point, rather than the minimization problem (REDUCED). It is in this sense that we consider (REDUCED) as a reformulation of the classical approach.

To compute the second derivative of $\bar{\Pi}$, we need the derivative of the functions $\tilde{\sigma}_m(\mu)$. However, in trying to differentiate (15) to obtain this, we realize that $\tilde{\sigma}_m(\mu)$ and $\tilde{\zeta}_m(\mu)$ are not differentiable when they are degenerate solutions of (IPPRIMAL), i.e., when $\varphi(\tilde{\sigma}_m(\mu), \tilde{\zeta}_m(\mu)) = 0$ and $\tilde{\lambda}_m(\mu) = 0^1$. In fact at

¹Indeed these degenerate points feature in the context of the first derivative (17) as well,

such points, these functions are only directionally differentiable [26]. When the minimizer of (REDUCED) is such a degenerate point, the rate of convergence of Newton's method is only super-linear rather than quadratic [27].

Here, we proceed formally ignoring these degenerate points, the set of which has measure zero in $\mathbb{R}^{N_{\text{DOF}}}$. We first introduce the index set

$$\mathcal{I}_m = \left\{ k \in \{1, \dots, N_y\} \mid (\lambda_m(\mu))_k > 0 \right\} \quad (19)$$

The optimality conditions (15) can then be rewritten as

$$\begin{aligned} \text{D}_1 \psi^c(\tilde{\sigma}_m(\mu), \tilde{\zeta}_m(\mu)) + \sum_{k \in \mathcal{I}_m} (\tilde{\lambda}_m(\mu))_k \text{D}_1 \varphi_k(\tilde{\sigma}_m(\mu), \tilde{\zeta}_m(\mu)) - (B_m \mu + b_{\sigma m})^\top &= 0 \\ \text{D}_2 \psi^c(\tilde{\sigma}_m(\mu), \tilde{\zeta}_m(\mu)) + \sum_{k \in \mathcal{I}_m} (\tilde{\lambda}_m(\mu))_k \text{D}_2 \varphi_k(\tilde{\sigma}_m(\mu), \tilde{\zeta}_m(\mu)) - b_{\zeta m}^\top &= 0 \\ \varphi_k(\tilde{\sigma}_m(\mu), \tilde{\zeta}_m(\mu)) &= 0, \text{ for } k \in \mathcal{I}_m \end{aligned}$$

Differentiating this, we get

$$\left[\begin{array}{c|c|c} K_{\sigma\sigma} & K_{\sigma\zeta} & \Phi_\sigma^\top \\ \hline K_{\sigma\zeta}^\top & K_{\zeta\zeta} & \Phi_\zeta^\top \\ \hline \Phi_\sigma & \Phi_\zeta & 0 \end{array} \right] \begin{pmatrix} \text{D}\tilde{\sigma}_m(\mu) \\ \text{D}\tilde{\zeta}_m(\mu) \\ \text{D}(\tilde{\lambda}_m(\mu)_{\mathcal{I}_m}) \end{pmatrix} = \begin{pmatrix} B_m \\ 0 \\ 0 \end{pmatrix} \quad (20a)$$

where

$$\begin{aligned} K_{\sigma\sigma} &= \text{D}_1^2 \psi^c(\tilde{\sigma}_m(\mu), \tilde{\zeta}_m(\mu)) + \sum_{k \in \mathcal{I}_m} (\tilde{\lambda}_m(\mu))_k \text{D}_1^2 \varphi_k(\tilde{\sigma}_m(\mu), \tilde{\zeta}_m(\mu)) \\ K_{\sigma\zeta} &= \text{D}_2 \text{D}_1 \psi^c(\tilde{\sigma}_m(\mu), \tilde{\zeta}_m(\mu)) + \sum_{k \in \mathcal{I}_m} (\tilde{\lambda}_m(\mu))_k \text{D}_2 \text{D}_1 \varphi_k(\tilde{\sigma}_m(\mu), \tilde{\zeta}_m(\mu)) \\ K_{\zeta\zeta} &= \text{D}_2^2 \psi^c(\tilde{\sigma}_m(\mu), \tilde{\zeta}_m(\mu)) + \sum_{k \in \mathcal{I}_m} (\tilde{\lambda}_m(\mu))_k \text{D}_2^2 \varphi_k(\tilde{\sigma}_m(\mu), \tilde{\zeta}_m(\mu)) \\ \Phi_\sigma &= \left(\text{D}_1 \varphi(\tilde{\sigma}_m(\mu), \tilde{\zeta}_m(\mu)) \right)_{\mathcal{I}_m} \\ \Phi_\zeta &= \left(\text{D}_2 \varphi(\tilde{\sigma}_m(\mu), \tilde{\zeta}_m(\mu)) \right)_{\mathcal{I}_m} \end{aligned} \quad (20b)$$

In the last two equations above, we have used MATLAB-style indexing [28].

The subscript \mathcal{I}_m : extracts the submatrix consisting of rows \mathcal{I}_m and all the

where an argument has to be made that $\tilde{\lambda}_m(\mu)^\top \text{D}\varphi = 0$ at such points.

columns.

The derivative $D\tilde{\sigma}_m(\mu)$ can be obtained by solving (20a). It is of the form $\bar{K}_m B_m$, where \bar{K}_m is referred to as the *consistent tangent stiffness* matrix [29]. When the submatrices in (20a) have a simple form, it may also be less expensive to compute the consistent tangent directly as

$$\bar{K}_m = K_{\sigma\sigma}^{-1} \left[K_{\sigma\sigma} + K_{\sigma\zeta} \bar{K}_{\zeta\zeta}^{-1} K_{\sigma\zeta}^\top - \bar{\Phi}_\sigma^\top \Xi^{-1} \bar{\Phi}_\sigma \right] K_{\sigma\sigma}^{-1} \quad (21a)$$

where

$$\begin{aligned} \bar{K}_{\zeta\zeta} &= K_{\zeta\zeta} - K_{\sigma\zeta}^\top K_{\sigma\sigma}^{-1} K_{\sigma\zeta} \\ \bar{\Phi}_\zeta &= \Phi_\zeta - \Phi_\sigma K_{\sigma\sigma}^{-1} K_{\sigma\zeta} \\ \bar{\Phi}_\sigma &= \Phi_\sigma - \bar{\Phi}_\zeta \bar{K}_{\zeta\zeta}^{-1} K_{\sigma\zeta}^\top \\ \Xi &= \Phi_\sigma K_{\sigma\sigma}^{-1} \Phi_\sigma^\top + \bar{\Phi}_\zeta \bar{K}_{\zeta\zeta}^{-1} \bar{\Phi}_\zeta^\top \end{aligned} \quad (21b)$$

Now, by differentiating equation (17), the second derivative of the objective function $\bar{\Pi}$, the tangent stiffness matrix, may be written as

$$\nabla^2 \bar{\Pi}(\mu) = \sum_{m=1}^{N_G} B_m^\top \bar{K}_m B_m \quad (22)$$

4.2. Optimization algorithm

With the first derivative $\nabla \bar{\Pi}(\mu)$, the vector of unbalanced forces, and second derivative $\nabla^2 \bar{\Pi}(\mu)$ the tangent stiffness matrix, at hand, the energy $\bar{\Pi}(\mu)$ can be minimized using the standard Newton's method for unconstrained minimization [21, 22], outlined in Procedure 1. A Newton direction $\delta\mu$ is computed by solving the linear system

$$\nabla^2 \bar{\Pi}(\mu^{\text{iter}}) \delta\mu = -\nabla \bar{\Pi}(\mu^{\text{iter}}) \quad (23)$$

To assure convergence for large increments, a line search is typically needed. A step length s is computed by backtracking to satisfy the following sufficient decrease condition.

$$\bar{\Pi}(\mu + s\delta\mu) \leq \bar{\Pi}(\mu) + \beta s \nabla \bar{\Pi}(\mu)^\top \delta\mu \quad (24)$$

where β is a sufficient decrease parameter to be in the interval $(0, 0.5)$ [21], taken in the example in section 6 as 10^{-4} . Solving the problem as one of optimization

removes the need to use any other heuristics to ensure convergence. The working of the backtracking procedure can be visualized as shown in Figure 4 in section 6.

Procedure 1 NEWTON'S METHOD FOR $\min \bar{\Pi}(\mu)$

```

1: Given force  $p$ , prescribed displacement  $\mu^{\text{prsc}}$ ,  $(b_{\sigma m}, b_{\zeta m})$  for each integration
   point  $m$ , and starting point  $\mu^0$ 
2: for iter  $\leftarrow 0, \text{MAXITER}$  do
3:   Compute  $\bar{\Pi}(\mu^{\text{iter}})$ ,  $\nabla \bar{\Pi}(\mu^{\text{iter}})$  and  $\nabla^2 \bar{\Pi}(\mu^{\text{iter}})$  using Procedure 2
4:   if  $\|\nabla \bar{\Pi}(\mu^{\text{iter}})\| \leq \text{tol}$  then
5:     break
6:   end if
7:   Compute search direction  $\delta\mu$  by solving (23)
8:    $s = 1$ 
9:   for nback  $\leftarrow 1, \text{MAXBACKTRACK}$  do ▷ backtracking line search
10:    Compute  $\bar{\Pi}(\mu^{\text{iter}} + s\delta\mu)$  using Procedure 2
11:    if sufficient decrease (24) is obtained then
12:      break
13:    end if
14:     $s \leftarrow \gamma s$  ▷  $\gamma$  is a backtracking parameter
15:  end for
16:   $\mu^{\text{iter}+1} \leftarrow \mu^{\text{iter}} + s\delta\mu$ 
17: end for

```

5. Solution of (IPPRIMAL) for specific constitutive models

In the framework described here, a constitutive model is specified by a complementary stored energy function ψ^c , and a yield function φ or complementary dissipation function ϕ^c . In general, (IPPRIMAL) may be solved (step 4 of Procedure 2) using any standard algorithm for inequality constrained convex optimization such as an interior-point method or a sequential quadratic

Procedure 2 EVALUATE $\bar{\Pi}(\mu)$, $\nabla\bar{\Pi}(\mu)$ AND $\nabla^2\bar{\Pi}(\mu)$

- 1: Given μ , p , μ^{prsc}
 - 2: $\bar{\Pi} \leftarrow -\mu^\top p$; $\nabla\bar{\Pi} \leftarrow -p$; $\nabla^2\bar{\Pi} \leftarrow 0$
 - 3: **for** $m \leftarrow 1, N_G$ **do**
 - 4: Compute $(\tilde{\sigma}_m, \tilde{\zeta}_m)$ by solving (IPPRIMAL)
 - 5: $\bar{\Pi} \leftarrow \bar{\Pi} - \left[\psi^c(\tilde{\sigma}_m, \tilde{\zeta}_m) - (B_m\mu + b_{\sigma m})^\top \tilde{\sigma}_m - b_{\zeta m}^\top \tilde{\zeta}_m \right]$
 - 6: Assemble $B_m^\top \tilde{\sigma}_m$ into $\nabla\bar{\Pi}$
 - 7: Computer \bar{K}_m using either of equations (20a) or (21a)
 - 8: Assemble $B_m^\top \bar{K}_m B_m$ into $\nabla^2\bar{\Pi}$
 - 9: **end for**
-

programming method [21, 22]. Alternately, it may also be advantageous on occasion to solve (IPDUAL), which has simple bound constraints. Such a general approach may often be necessary, particularly for more complex models such as multi-surface plasticity models. However in some cases, specific forms of the complementary stored energy function ψ^c and the yield function φ may facilitate simpler strategies to solve (IPPRIMAL). These strategies are known as return-mapping algorithms. In the following, we discuss one such case, namely an elastoplastic model characterized by isotropic linear elasticity, linear kinematic hardening, nonlinear isotropic hardening, and von Mises yield condition. This model is described by

$$\begin{aligned} \psi^c(\sigma, \zeta) &= \frac{1}{2} \sigma^\top C^{-1} \sigma + \frac{1}{2} \zeta_{\text{kh}}^\top H^{-1} \zeta_{\text{kh}} + \psi_{\text{ih}}^c(\zeta_{\text{ih}}) \\ \varphi(\sigma, \zeta) &= \sqrt{(\sigma - \zeta_{\text{kh}})^\top P (\sigma - \zeta_{\text{kh}})} - \sqrt{\frac{2}{3}} (\sigma_y + \zeta_{\text{ih}}) \end{aligned} \quad (25)$$

Here, ζ_{kh} and ζ_{ih} are components of the internal variable ζ corresponding to kinematic hardening and isotropic hardening respectively. ζ_{kh} is often referred to as the back stress, and is the same type of object as σ . ζ_{kh} is a scalar. C and H are matrices of elastic and kinematic hardening moduli. The quadratic terms in ψ^c correspond to linear elasticity and linear kinematic hardening. The function ψ_{ih}^c is not necessarily quadratic, and represents nonlinear isotropic hardening. The relationship between this form of ψ^c and the hardening model discussed in

[15] is discussed in [1]. von Mises yield function in both 3D and 2D plane-stress cases can be expressed in the form φ above with appropriate choice of the matrix P (Table 1) [15]. σ_y is the uniaxial yield stress.

The optimality conditions (15) corresponding to the model (25) are

$$\begin{aligned}
C^{-1}\sigma + \lambda \frac{P(\sigma - \zeta_{kh})}{\sqrt{(\sigma - \zeta_{kh})^\top P(\sigma - \zeta_{kh})}} - (B\mu + b_\sigma) &= 0 \\
H^{-1}\zeta_{kh} - \lambda \frac{P(\sigma - \zeta_{kh})}{\sqrt{(\sigma - \zeta_{kh})^\top P(\sigma - \zeta_{kh})}} - b_{\zeta_{kh}} &= 0 \\
\psi_{ih}^c{}'(\zeta_{ih}) - \lambda \sqrt{\frac{2}{3}} - b_{\zeta_{ih}} &= 0 \\
\varphi(\sigma, \zeta) \leq 0, \quad \lambda \geq 0, \quad \lambda \varphi(\sigma, \zeta) &= 0
\end{aligned} \tag{26}$$

where the prime on ψ_{ih}^c denotes the first derivative. For brevity, we have written σ for $\tilde{\sigma}_m(\mu)$ etc. and dropped the subscript m . Since there is a single yield condition, there are only two possibilities.

1. $\varphi(\sigma, \zeta) \leq 0$. In this case, the material point is elastic in the increment, and $\lambda = 0$ from equation (26)₄. From equations (26)_{1,2,3}, an *elastic trial state* is computed.

$$\sigma^{\text{trial}} = \sigma^n + CB\mu, \quad \zeta_{kh}^{\text{trial}} = \zeta_{kh}^n, \quad \zeta_{ih}^{\text{trial}} = \zeta_{ih}^n \tag{27}$$

If $\varphi(\sigma^{\text{trial}}, \zeta^{\text{trial}}) \leq 0$ then this is the solution of (IPPRIMAL).

2. If $\varphi(\sigma^{\text{trial}}, \zeta^{\text{trial}}) > 0$, it can be concluded the material point plastifies. So $\lambda > 0$, and (26)_{1,2,3,4} constitute four equations in the four unknowns σ , ζ_{kh} , ζ_{ih} and λ . To solve these, a further property of the matrices involved may be invoked. In both 3D and 2D plane-stress cases, the matrices C , H and P share the same eigenvectors. Therefore, there is an orthogonal matrix Q (Table 1), consisting of these eigenvectors as columns, which simultaneously diagonalizes all three matrices, i.e. $Q^\top P Q$ is diagonal matrix Λ_P etc. This has been pointed out for the 2D case in [30]. The 3D case is generally presented differently, by decomposing the stress into volumetric and deviatoric parts. In both cases, however, Q represents transformation of stress components to volumetric-deviatoric coordinates. Equations

		P	Q
3D	$\frac{1}{3}$	$\begin{bmatrix} 2 & -1 & -1 & 0 & 0 & 0 \\ -1 & 2 & -1 & 0 & 0 & 0 \\ -1 & -1 & 2 & 0 & 0 & 0 \\ 0 & 0 & 0 & 6 & 0 & 0 \\ 0 & 0 & 0 & 0 & 6 & 0 \\ 0 & 0 & 0 & 0 & 0 & 6 \end{bmatrix}$	$\begin{bmatrix} \frac{1}{\sqrt{3}} & \sqrt{\frac{2}{3}} & 0 & 0 & 0 & 0 \\ \frac{1}{\sqrt{3}} & -\frac{1}{\sqrt{6}} & \frac{1}{\sqrt{2}} & 0 & 0 & 0 \\ \frac{1}{\sqrt{3}} & -\frac{1}{\sqrt{6}} & -\frac{1}{\sqrt{2}} & 0 & 0 & 0 \\ 0 & 0 & 0 & 1 & 0 & 0 \\ 0 & 0 & 0 & 0 & 1 & 0 \\ 0 & 0 & 0 & 0 & 0 & 1 \end{bmatrix}$
2D plane-stress	$\frac{1}{3}$	$\begin{bmatrix} 2 & -1 & 0 \\ -1 & 2 & 0 \\ 0 & 0 & 6 \end{bmatrix}$	$\begin{bmatrix} \frac{1}{\sqrt{2}} & \frac{1}{\sqrt{2}} & 0 \\ \frac{1}{\sqrt{2}} & -\frac{1}{\sqrt{2}} & 0 \\ 0 & 0 & 1 \end{bmatrix}$

Table 1: von Mises yield condition matrix P and diagonalizing matrix Q

(26)_{1,2,3,4} can be rewritten as

$$\begin{aligned}
\sigma + \frac{\lambda}{\sqrt{\frac{2}{3}}(\sigma_y + \zeta_{ih})} CP(\sigma - \zeta_{kh}) - \sigma^{\text{trial}} &= 0 \\
\zeta_{kh} - \frac{\lambda}{\sqrt{\frac{2}{3}}(\sigma_y + \zeta_{ih})} HP(\sigma - \zeta_{kh}) - \zeta_{kh}^{\text{trial}} &= 0 \\
\psi_{ih}^{\prime}(\zeta_{ih}) - \lambda \sqrt{\frac{2}{3}} - b_{\zeta_{ih}} &= 0 \\
\sqrt{(\sigma - \zeta_{kh})^\top P(\sigma - \zeta_{kh})} &= \sqrt{\frac{2}{3}}(\sigma_y + \zeta_{ih})
\end{aligned} \tag{28}$$

where $b_{\zeta_{ih}}$ is the component b_ζ corresponding to ζ_{ih} . Introducing the coordinate transformation $\sigma = Qy_\sigma$ and $\zeta_{kh} = Qy_{\zeta_{kh}}$, subtracting (28)₂ from (28)₁, and multiplying through from the left by Q^\top , we have

$$y_\sigma - y_{\zeta_{kh}} = \left(I + \frac{\lambda}{\sqrt{\frac{2}{3}}(\sigma_y + \zeta_{ih})} \Lambda_{(C+H)P} \right)^{-1} Q^\top (\sigma^{\text{trial}} - \zeta_{kh}^{\text{trial}}) \tag{29}$$

where the diagonal matrix $\Lambda_{(C+H)P} = Q^\top (C + H) P Q$. Solving equation

(28)₃ for λ and substituting, we get

$$y_\sigma - y_{\zeta_{\text{kh}}} = \left(I + \frac{3}{2} \frac{\psi_{\text{ih}}^c{}'(\zeta_{\text{ih}}) - b_{\zeta_{\text{ih}}}}{\sigma_y + \zeta_{\text{ih}}} \Lambda_{(C+H)P} \right)^{-1} Q^\top (\sigma^{\text{trial}} - \zeta_{\text{kh}}^{\text{trial}})$$

Lastly, substituting this in (28)₄ and squaring, we get the following scalar equation for ζ_{ih} .

$$\sum_r (\Lambda_P)_r \left(\frac{[Q^\top (\sigma^{\text{trial}} - \zeta_{\text{kh}}^{\text{trial}})]_r}{\sqrt{\frac{2}{3}}(\sigma_y + \zeta_{\text{ih}}) + \sqrt{\frac{3}{2}}(\psi_{\text{ih}}^c{}'(\zeta_{\text{ih}}) - b_{\zeta_{\text{ih}}})(\Lambda_{(C+H)P})_r} \right)^2 = 1 \quad (30)$$

where r goes from 1 to 6 in 3D and from 1 to 3 in 2D. Equation (30) can also be written equivalently as

$$\sum_r (\Lambda_P)_r \left(\frac{[Q^\top (\sigma^{\text{trial}} - \zeta_{\text{kh}}^{\text{trial}})]_r}{\sqrt{\frac{2}{3}}(\sigma_y + \psi_{\text{ih}}^c{}'(\alpha_{\text{ih}})) + \sqrt{\frac{3}{2}}(\alpha_{\text{ih}} - b_{\zeta_{\text{ih}}})(\Lambda_{(C+H)P})_r} \right)^2 = 1 \quad (31)$$

where α_{ih} is the kinematic internal state for isotropic hardening, and ψ_{ih} is the Legendre transform of ψ_{ih}^c . α_{ih} is the equivalent plastic strain [1]. Equation (31) is a scalar non-linear equation in α_{ih} , which can be solved by Newton's method. The other states can then be calculated as summarized in Procedure 3.

The consistent tangent can be calculated using (21). The above process of solving (IPPRIMAL) for the constitutive model (25) is summarized in Procedure 3.

We recount that a simpler strategy to solve (IPPRIMAL) for the constitutive model (25) is enabled by the following features.

1. The model has only one yield condition
2. σ and ζ are uncoupled in the complementary stored energy function ψ^c
3. The part of ζ that appears in a non-quadratic manner in ψ^c , namely the isotropic hardening state ζ_{ih} , is a scalar. This helps in reducing the problem to a scalar equation as in (31).

4. C , H and P share the same eigenvectors, so that there is a diagonalizing coordinate transformation Q .

In addition, in the 3D case, $(\Lambda_P)_1 = 0$ since the von Mises yield constraint applies to the deviatoric part of the stress, and $(\Lambda_{(C+H)P})_{2:6} = 2(G + G_{\text{kh}})$ where G and G_{kh} are the elastic and kinematic hardening shear moduli. The solution of (IPPRIMAL) can also be interpreted as a radial projection of the trial state on the elastic region, and is referred to as radial return mapping [15, 29]. In the 2D plane stress case, squaring the yield condition as done in [30] further simplifies the expression for the consistent tangent. However, here we keep the yield function as shown in $(25)_2$, so that it remains a convex function and so that the 3D and plane stress cases can be treated in a uniform manner. We also note that if isotropic hardening were also linear, then the objective function in (IPPRIMAL) can be written as

$$\frac{1}{2}(\sigma - \sigma^{\text{trial}})^\top C^{-1}(\sigma - \sigma^{\text{trial}}) + \frac{1}{2}(\zeta - \zeta^{\text{trial}})^\top H^{-1}(\zeta - \zeta^{\text{trial}})$$

Thus the solution can be interpreted as the closest point projection in the C^{-1}, H^{-1} norm of the trial state on the elastic region. In the absence of such simplifying features, (IPPRIMAL) must be solved by a general constrained convex optimization strategy.

6. Numerical example

In this section, we present a numerical example to illustrate the application of Procedure 1. We use a finite element model of a plate with a circular hole subject to uniform extension at the end, considered by Simo and Taylor [30]. Due to symmetry, only a quarter of the plate needs to be represented as shown in Figure 2. In order to compare the numerical solution and convergence characteristics, we use the same displacement-based finite element and discretization as used in this reference. We note however, that the formulation presented in this paper can be used with other finite element types. A constitutive model characterized by linear elasticity, linear isotropic hardening, and a single von Mises' yield

Procedure 3 SOLUTION OF (IPPRIMAL) FOR CONSTITUTIVE MODEL (25)

 (RETURN MAP)

- 1: Given $\sigma^n, \zeta_{\text{kh}}^n, \zeta_{\text{ih}}^n, \mu$
 - 2: Compute $\sigma^{\text{trial}} = \sigma^n + CB\mu, \zeta_{\text{kh}}^{\text{trial}} = \zeta_{\text{kh}}^n$ and $\zeta_{\text{ih}}^{\text{trial}} = \zeta_{\text{ih}}^n$
 - 3: **if** $\varphi(\sigma^{\text{trial}}, \zeta^{\text{trial}}) \leq 0$ **then**
 - 4: $\sigma = \sigma^{\text{trial}}, \zeta = \zeta^{\text{trial}}, \lambda = 0$
 - 5: $\bar{K} = C$
 - 6: **else**
 - 7: Compute $Q^\top(\sigma^{\text{trial}} - \zeta^{\text{trial}})$
 - 8: Solve (31) for α_{ih}
 - 9: $\zeta_{\text{ih}} = \psi_{\text{ih}}'(\alpha_{\text{ih}})$
 - 10: Calculate λ using (28)₃
 - 11: Compute σ and ζ_{kh} from equation (28)_{1,2}
 - 12: Calculate \bar{K} using equation (21)
 - 13: **end if**
-

function, is used to represent material behavior. This is a special case of the material model (25) with $\psi_{\text{ih}}^c(\zeta_{\text{ih}}) = \frac{1}{2}h^{-1}\zeta_{\text{ih}}^2$. Thus the Procedure 3 can be used to solve (IPPRIMAL). Material properties are chosen following [30] as $E = 70$, $\nu = 0.2$, $\sigma_y = 0.243$ and $h = 2.24$, where E is Young's modulus and ν is Possion's ratio. Extension is applied to the plate by imposing a uniform displacement at the top edge of the plate. Of the three sequences of increments considered in reference [30], we only present results for the most challenging case, where two displacements increments of size 0.5 are applied in succession. In Procedure 2, the backtracking parameters are taken as $\beta = 10^{-4}$ and $\gamma = 0.5$.

Table 2 shows norms of the residuals that arise in applying the optimization algorithm of Procedure 1 for each increment. The approximate doubling of significant digits in the residuals in later iterations suggests quadratic rate of convergence. The table also shows the step length used in each iteration, from which we see that at most two backtracking steps used and that the full Newton

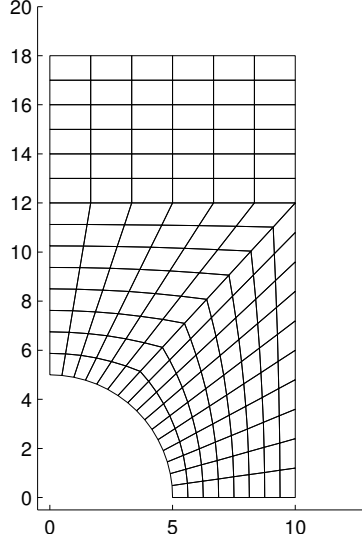


Figure 2: Finite element model of a plate with circular hole

step is always used in the last several iterations. The performance is comparable to that reported in [30], with fewer backtracking steps used attributable to use of the sufficient decrease condition. The von Mises stress computed and the spread of plasticity are shown in Figure 3.

A typical backtracking process used to obtain the step length is depicted in Figure 4. Such plots represent cross-sections along the Newton search path, and show the following as functions of the step length s .

1. Objective function, $\bar{\Pi}(\mu + s\delta\mu)$
2. First order approximation, $\bar{\Pi}(\mu) + s\nabla\bar{\Pi}(\mu)^\top\delta\mu$
3. Second order approximation, $\bar{\Pi}(\mu) + s\nabla\bar{\Pi}(\mu)^\top\delta\mu + \frac{1}{2}s^2\delta\mu^\top\nabla^2\bar{\Pi}(\mu)\delta\mu$
4. Sufficient descent criterion, $\bar{\Pi}(\mu) + \beta s\nabla\bar{\Pi}(\mu)^\top\delta\mu$

These plots illustrate the working of the backtracking search, as well as serve to check derivative computations during implementation. In Figure 4a, the iterate is far away from the solution. Thus the objective function deviates considerably from its second order approximation, and a step length of 0.5 is required to satisfy the sufficient decrease condition (24). On the other hand in Figure

Iteration	Increment (Step Length)	
	1	2
1	6.66e+00	5.93e+00
2	2.18e+00	1.44e+00 (0.5)
3	1.38e+00 (0.25)	6.80e-01 (0.5)
4	1.57e+00 (0.5)	7.00e-01 (0.5)
5	1.33e+00 (0.25)	5.33e-01 (0.25)
6	1.12e+00 (0.25)	3.43e-01 (0.5)
7	8.59e-01	1.34e-01
8	3.96e-01 (0.5)	3.12e-02
9	1.75e-01	9.63e-03
10	2.06e-02	8.87e-04
11	1.53e-03	2.45e-06
12	6.15e-06	1.89e-11
13	1.42e-10	

Table 2: Norm of of unbalanced force, $||\nabla \bar{\Pi}(\mu)||$

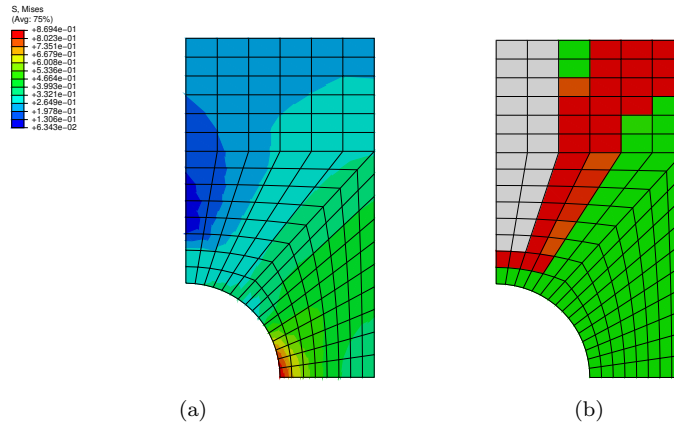


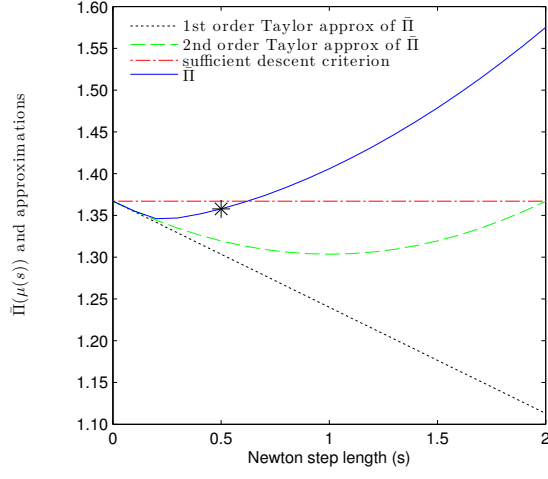
Figure 3: Numerical example (a) von Mises stress, $\sqrt{\sigma^\top P \sigma}$, after increment 2 (b) Spread of plasticity (green — yielded in increment 1; red — yielded in increment 2; orange — some integration points yielded in increment 2)

4b, the iterate is close the solution, the second order approximation closely follows the function, and the full Newton step is taken. We note that because of the optimization reformulation, we are able to select the step length based on sufficient decrease of the objective function, rather than on heuristics such as number of iterations. In this example, despite the rather large displacement increments, at most two backtracking steps are needed in any iteration as seen from Table 2.

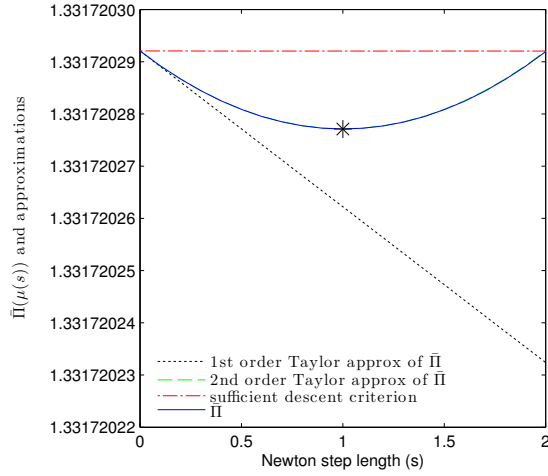
7. Relationships with other approaches

In section 3, we derived three equivalent optimization problems for incremental state update — a primal problem (PRIMAL), the dual problem (DUAL), and a reduced dual problem (REDUCED). In the present section, we briefly review relationships these problems share with other approaches recently presented in the literature.

There has been recent work on solving the primal problem in the context of quasi-static elastoplastic models. Krabbenhoft et al. [23] arrive at the primal problem through a different route, and solve it directly by an interior point method. Bilotta et al. [24] also solve the primal problem directly, but by a sequential quadratic programming (SQP) approach. Wieners [31] solves a KKT system similar to (6) by SQP. When ψ^c is quadratic (corresponding to linear elastic and linear hardening models), and when the yield function is of the form of a 2-norm (as is the case with the von Mises function in section 5), then (7) can be recast as a second order cone program (SOCP) [32]. This can in turn be reformulated as a semi-definite program (SDP) [33], which can be solved by efficient interior point methods that have been recently developed. Krabbenhoft et al. [14, 34] also use this approach to approximate a non-associated flow model by a convex one. Sivaselvan et al. [25] solve a primal-type problem that arises in dynamics problems. Further relationships to dynamic problems are discussed in [1]. In all of these primal approaches, a concept similar to the Sherman-Morrison-Woodbury formula is used to reduce the linear system to be solved



(a) Increment 2, iteration 2



(b) Increment 2, iteration 10

Figure 4: Visualization of backtracking for step length determination

[25]. Bilotta et al. [24] discuss the relationship between the primal optimization problem and the displacement-based nested approach through the dual problem, albeit lightly differently than done in this paper. In [35], the KKT conditions are solved directly as a mixed complementarity problem (MCP).

As noted in section 4.1, equation (18) can also be obtained directly from (6),

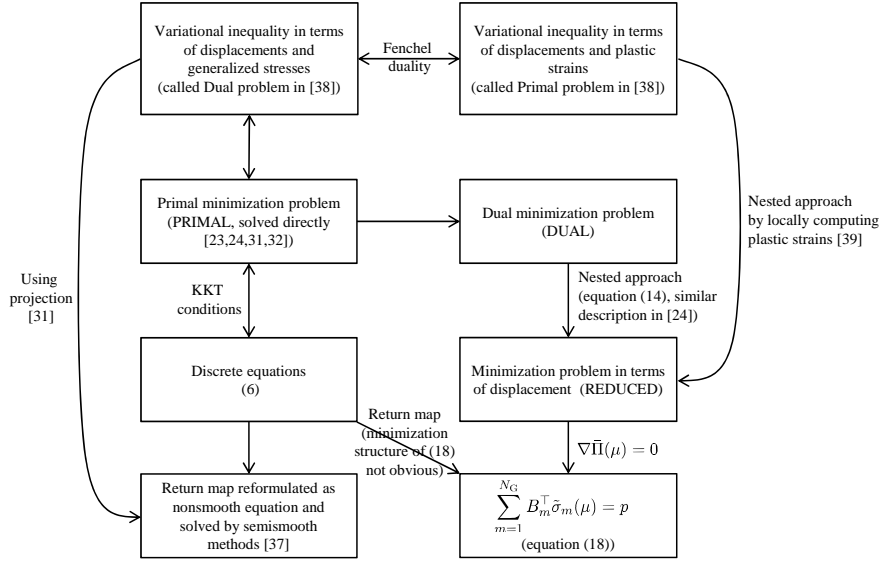


Figure 5: Interrelation of various approaches to elastoplastic problems using optimization

since $(6)_{1,2,4}$ are the KKT conditions of (IPPRIMAL). However, when viewed in this manner, the minimization structure at the global level is not apparent. In the context of plasticity models, $(\tilde{\sigma}_m(\mu), \tilde{\zeta}_m(\mu))$ is referred to as a *return map*. As discussed at the end of section 5, for certain classes of problems, the return map defined by (IPPRIMAL) can be viewed as a *projection* [15, 31]. Other approaches are also possible, for example local problem is considered as a linear complementarity problem (LCP) in [36]. Following the seminal paper [29], Newton's method has been successfully applied to solve (18) in many cases. However, since the return map is not differentiable, convergence properties of Newton's method cannot be rigorously established. Consequently, *semismooth* methods have been presented together with convergence analyses [37].

Optimization problems for quasi-static elastoplasticity can also be derived starting from variational inequality formulations presented for example by Han and Reddy [38]. An optimization problem developed in this manner in terms of displacements μ and kinematic internal states or plastic strains α is considered

by Alberty et al. [39]. They use the optimization structure to develop error measures and an adaptive mesh-refining strategy. Gruber and Valdman [40] derive a minimization problem of the form (REDUCED) for a class of elastoplastic models again starting from a variational inequality. They prove the differentiability of a function similar to $\bar{\Pi}$ using the Moreau-Yosida theorem. Recognizing that the second derivative is not continuous, as discussed in section 4.1, they use a slant Newton method. Some of the interrelations described above are shown schematically in Figure 5.

8. Concluding remarks

We take a mathematical programming approach to the incremental state update of non-linear mechanics models with material behavior described by stored energy and dissipation function. In the case where these energy functions are convex and of a specific form (equation (2)), the classical displacement-based nested approach can be reformulated as a reduced dual optimization problem (REDUCED). We have presented an optimization reformulation of the classical displacement-based nested approach to incremental state update. This reformulation allows visualizing the working of the algorithm by means of geometrical constructions such as Figure 4, and further illustrates the unifying nature of the mathematical programming approach to state update. Connections with related algorithms recently presented in the literature have also been discussed. We envision that such understanding gained will aid in developing algorithms for more complex non-linear material models, such as those involving non-associated flow, softening etc., for example by means of successive optimization strategies.

NOTATION

B	Linearized strain-displacement matrix ($\in \mathbb{R}^{N_\sigma N_G \times N_{\text{DOF}}}$)
B_m	Rows of the matrix B corresponding to integration point m ($\in \mathbb{R}^{N_\sigma \times N_{\text{DOF}}}$)

B^{prsc}	Deformation-displacement matrix associated with DOF with prescribed displacement
C_d	Damping matrix ($\in \mathbb{R}^{N_{\text{DOF}} \times N_{\text{DOF}}}$)
C	Matrix of elastic moduli in the constitutive model equation (25)
\mathcal{C}	Convex elastic region
D, D_q	Derivative of a differentiable function; subscript q denotes with respect to argument q
E	Young's modulus (used in the numerical examples)
\mathcal{E}	Nonlinear deformation-displacement map used only in the remarks following equation (1)
G, G_{kh}	Elastic and kinematic hardening shear moduli used only at the end of section 5
H	Matrix of kinematic hardening moduli in the constitutive model equation (25)
I	Identity matrix of appropriate size
\mathcal{I}_m	Index set of activated yield conditions defined in equation (19)
$K_{\sigma\sigma}, K_{\sigma\zeta}, K_{\zeta\zeta}$	Derivative matrices defined in equation (20b)
\bar{K}_m	Consistent tangent stiffness matrix for integration point m
$\bar{K}_{\zeta\zeta}$	Derivative matrix defined in equation (21b)
\mathcal{L}	Lagrangian of the primal optimization problem (equation (9))
\mathcal{L}_m	Contribution to primal Lagrangian of integration point m (equation (10))
M	Mass matrix ($\in \mathbb{R}^{N_{\text{DOF}} \times N_{\text{DOF}}}$)
MAXBACKTRACK	Maximum number of backtracking steps in Procedure 1
MAXITER	Maximum number of Newton iterations in Procedure 1
N_{DOF}	Number of free degrees of freedom
N_G	Number of integration points

N_σ	Number of stress components per material point (for example, 3 in 2D problems and 6 in 3D problems)
N_ζ	Number of internal variables per material point (for example, 4 for 2D elastoplasticity with one yield condition and combined isotropic and kinematic hardening)
P	Matrix in von Mises yield condition (25) ₂
$\bar{\Phi}_\sigma, \bar{\Phi}_\zeta$	Derivative matrices defined in equation (21b)
Q	Diagonalizing coordinate transformation matrix (Table 1)
Δt	Time increment
Λ_\square	Diagonal matrix containing the eigenvalues of the symmetric matrix \square , used in equation (30)
Φ_σ, Φ_ζ	Derivative matrices defined in equation (20b)
Π	Objective function of dual problem, defined in equation (11), explicit formula in equation (13)
$\bar{\Pi}$	Objective function of the reduced dual problem defined in equation (14)
Π^c	Objective function of the primal optimization problem (equation (8))
Ξ	Derivative matrix defined in equation (21b)
α	Kinematic internal variable at a material point
α_{ih}	Isotropic hardening internal state conjugate to ζ_{kh} , used in equation (31)
β	Sufficient decrease parameter used in choice of step length (equation (24))
$\delta\mu$	Newton search direction (equation (23))
ϵ	Strain at a material point
γ	Backtracking parameter used in Procedure 1
λ, λ_m	Vector of equivalent plastic strain increments for the entire model ($\in \mathbb{R}^{N_y N_G}$), or for a single material point ($\in \mathbb{R}^{N_y}$)

$\bar{\lambda}, \bar{\lambda}^{n+1}$	Vector in equations (3) and (4) ($\in \mathbb{R}^{N_y}$); corresponds to equivalent plastic strain rate; superscript denotes time increment index
$\tilde{\lambda}_m$	Minimizer of (IPDUAL)
μ	Incremental displacement, $u^{n+1} - u^n$
μ^{iter}	μ in iteration number iter of Newton's method (Procedure 1)
μ^{prsc}	Increment of prescribed displacement
ν	Poisson's ratio (used in the numerical examples)
ϕ	Dissipation function for a material point
ϕ^c	Complementary dissipation function for a material point, or for entire model, depending on context
φ	Yield function
ψ	Stored energy function for a material point
ψ^c	Complementary stored energy function for a material point, or for entire model, depending on context
ψ_{ih}^c	Part of complementary stored energy representing kinematic hardening in the constitutive model equation (25)
ψ_{ih}	Legendre transform of ψ_{ih}^c , used in equation (31)
$\sigma, \sigma^n, \sigma^{n+1}, \sigma_m$	Stress at a material point ($\in \mathbb{R}^{N_\sigma}$) or collection over all material points ($\in \mathbb{R}^{N_\sigma N_G}$) depending on context; superscripts denote time increment index, and subscripts material point index
$\tilde{\sigma}_m$	Minimizer of (IPPRIMAL)
σ^{trial}	Elastic trial stress (equation (27))
σ_y	Uniaxial yield stress in von Mises yield condition (25) ₂
σ_m^*	Minimizer of equation (11) defined implicitly in equations (12)
$\zeta, \zeta^n, \zeta^{n+1}, \zeta_m$	Generalized stress internal variable at a material point ($\in \mathbb{R}^{N_\zeta}$) or collection over all material points ($\in \mathbb{R}^{N_\zeta N_G}$) depending on

	context; superscripts denote time increment index, and subscripts material point index
$\zeta_{\text{kh}}, \zeta_{\text{ih}}$	Components of internal variable ζ corresponding to kinematic and isotropic hardening, used in constitutive model equation (25)
ζ_m^*	Minimizer of equation (11) defined implicitly in equations (12)
$\tilde{\zeta}_m$	Minimizer of (IPPRIMAL)
$\zeta^{\text{trial}}, \zeta_{\text{kh}}^{\text{trial}}, \zeta_{\text{ih}}^{\text{trial}}$	Elastic trial state (equation (27))
$b_\sigma, b_{\sigma m}$	Defined in equation (6); components of b_σ corresponding to integration point m
$b_\zeta, b_{\zeta m}$	Defined in equation (6); components of b_ζ corresponding to integration point m
$b_{\zeta_{\text{kh}}}, b_{\zeta_{\text{ih}}}$	Components of b_ζ corresponding to ζ_{kh} and ζ_{ih} , used following equation (26) in section 5
h	Isotropic hardening modulus used in the numerical example
iter	Iteration count in Newton's method in Procedure 1
k	Yield function component index within an integration point $\in \{1, \dots, N_y\}$
m	Integration point index $\in \{1, \dots, N_G\}$
n	Time increment index
nback	Number of backtracking steps in Procedure 1
p, p^{n+1}	External load vector, and its values at time $n+1$ ($\in \mathbb{R}^{N_{\text{DOF}}}$)
r	Index used in equation (30)
s	Length of Newton step in 1
t	Time
tol	Convergence tolerances for Newton's method in Procedure 1
u, u^n, u^{n+1}	Displacement at free DOF, and its values at times n and $n+1$ ($\in \mathbb{R}^{N_{\text{DOF}}}$)

v, v^n, v^{n+1}	Velocities at free DOF, and its values at times n and $n + 1$ ($\in \mathbb{R}^{N_{\text{DOF}}}$)
x	Generic variable used in Figure 1
$y_\sigma, y_{\zeta_{\text{kh}}}$	Components of stress and kinematic hardening internal state in volumetric-deviatoric coordinates
∇, ∇_q	Gradient of a differentiable function; subscript q denotes with respect to argument q
∂, ∂_q	Subdifferential of a nonsmooth convex function; subscript q denotes with respect to argument q
$\sqcup_{\mathcal{C}}$	Indicator function of the convex elastic region \mathcal{C}

References

- [1] M. V. Sivaselvan, Hysteretic models with stiffness and strength degradation in a mathematical programming format, *International Journal of Non-Linear Mechanics* 51 (2013) 10–27.
- [2] B. Halphen, S. Nguyen Quoc, Sur les matériaux standard généralisés, *Journal de Mécanique* 14 (1) (1975) 39–63.
- [3] G. T. Houlsby, A. M. Puzrin, *Principles of hyperplasticity : an approach to plasticity theory based on thermodynamic principles*, Springer, London, 2006.
- [4] S. Erlicher, N. Point, Endochronic theory, non-linear kinematic hardening rule and generalized plasticity: a new interpretation based on generalized normality assumption, *International Journal of Solids and Structures* 43 (14-15) (2006) 4175–200.
- [5] F. Preisach, Über die magnetische nachwirkung, *Zeitschrift für Physik* 94 (5-6) (1935) 277–302.

- [6] P. D. Spanos, A. Kontsos, P. Cacciola, Steady-state dynamic response of preisach hysteretic systems, *Journal of Vibration and Acoustics-Transactions of the ASME* 128 (2) (2006) 244–250.
- [7] R. Bouc, Mathematical model for hysteresis, *Acustica* 24 (1) (1971) 16–25.
- [8] Y. K. Wen, Method for random vibration of hysteretic systems, *Journal of the Engineering Mechanics Division-ASCE* 102 (2) (1976) 249–263.
- [9] S. Erlicher, O. S. Bursi, Bouc-Wen-type models with stiffness degradation: Thermodynamic analysis and applications, *Journal of Engineering Mechanics-ASCE* 134 (10) (2008) 843–855.
- [10] M. Ismail, F. Ikhoulane, J. Rodellar, The hysteresis bouc-wen model, a survey, *Archives of Computational Methods in Engineering* 16 (2) (2009) 161–188.
- [11] M. Anitescu, G. D. Hart, Solving nonconvex problems of multibody dynamics with joints, contact, and small friction by successive convex relaxation, *Mechanics Based Design of Structures and Machines* 31 (3) (2003) 335–356.
- [12] G. Garcea, L. Leonetti, A unified mathematical programming formulation of strain driven and interior point algorithms for shakedown and limit analysis, *International Journal for Numerical Methods in Engineering* 88 (11) (2011) 1085–1111.
- [13] G. Milani, A. Tralli, Simple sqp approach for out-of-plane loaded homogenized brickwork panels, accounting for softening, *Computers and Structures* 89 (1-2) (2011) 201–215.
- [14] K. Krabbenhoft, M. R. Karim, A. V. Lyamin, S. W. Sloan, Associated computational plasticity schemes for nonassociated frictional materials, *International Journal for Numerical Methods in Engineering* 90 (9) (2012) 1089–1117.

- [15] J. C. Simo, T. J. R. Hughes, Computational inelasticity, Springer, New York, 1998.
- [16] A. Mielke, A mathematical framework for generalized standard materials in the rate-independent case, in: Multifield Problems in Solid and Fluid Mechanics, Springer, 2006, pp. 399–428.
- [17] I. F. Collins, G. T. Houlsby, Application of thermomechanical principles to the modelling of geotechnical materials, Proceedings of the Royal Society of London Series A-Mathematical Physical and Engineering Sciences 453 (1964) (1997) 1975–2001.
- [18] J. M. Borwein, A. S. Lewis, Convex analysis and nonlinear optimization : theory and examples, 2nd Edition, Springer, New York, 2006.
- [19] M. V. Sivaselvan, A. M. Reinhorn, Lagrangian approach to structural collapse simulation, Journal of Engineering Mechanics-ASCE 132 (8) (2006) 795–805.
- [20] S. Erlicher, N. Point, On the associativity of the Drucker-Prager model, in: E. Oñate, D. Owen (Eds.), VIII International Conference on Computational Plasticity COMPLAS VIII, Barcelona, 2005.
- [21] J. Nocedal, S. J. Wright, Numerical optimization, 2nd Edition, Springer, New York, 2006.
- [22] S. P. Boyd, L. Vandenberghe, Convex optimization, Cambridge University Press, Cambridge ; New York, 2004.
- [23] K. Krabbenhoft, A. V. Lyamin, S. W. Sloan, P. Wriggers, An interior-point algorithm for elastoplasticity, International Journal for Numerical Methods in Engineering 69 (3) (2007) 592–626.
- [24] A. Bilotta, L. Leonetti, G. Garcea, An algorithm for incremental elastoplastic analysis using equality constrained sequential quadratic programming, Computers and Structures 102 (2012) 97–107.

- [25] M. V. Sivaselvan, O. Lavan, G. F. Dargush, H. Kurino, Y. Hyodo, R. Fukuda, K. Sato, G. Apostolakis, A. M. Reinhorn, Numerical collapse simulation of large-scale structural systems using an optimization-based algorithm, *Earthquake Engineering & Structural Dynamics* 38 (5) (2009) 655–677.
- [26] S. Dempe, Directional differentiability of optimal solutions under slater’s condition, *Mathematical Programming* 59 (1-3) (1993) 49–69.
- [27] L. Qi, J. Sun, A nonsmooth version of newton’s method, *Mathematical Programming* 58 (1-3) (1993) 353–367.
- [28] The Mathworks Inc., MATLAB Version 7.8.0.347 (R2009a) (2009).
- [29] J. C. Simo, R. L. Taylor, Consistent tangent operators for rate-independent elastoplasticity, *Computer Methods in Applied Mechanics and Engineering* 48 (1) (1985) 101–118.
- [30] J. C. Simo, R. L. Taylor, A return mapping algorithm for plane stress elastoplasticity, *International Journal for Numerical Methods in Engineering* 22 (3) (1986) 649–670.
- [31] C. Wieners, Nonlinear solution methods for infinitesimal perfect plasticity, *ZAMM - Journal of Applied Mathematics and Mechanics / Zeitschrift für Angewandte Mathematik und Mechanik* 87 (8-9) (2007) 643–660.
- [32] K. Yonekura, Y. Kanno, Second-order cone programming with warm start for elastoplastic analysis with von mises yield criterion, *Optimization and Engineering* 13 (2) (2012) 181–218.
- [33] A. Antoniou, W. Lu, Practical optimization : algorithms and engineering applications, Springer, New York, 2007.
- [34] K. Krabbenhoft, A. V. Lyamin, Computational cam clay plasticity using second-order cone programming, *Computer Methods in Applied Mechanics and Engineering* 209 (2012) 239–249.

- [35] S. Tangaramvong, F. Tin-Loi, C. Song, A direct complementarity approach for the elastoplastic analysis of plane stress and plane strain structures, *International Journal for Numerical Methods in Engineering* 90 (7) (2012) 838–866.
- [36] A. Bassi, N. Aravas, F. Genna, A linear complementarity formulation of rate-independent finite-strain elastoplasticity. part I: Algorithm for numerical integration, *European Journal of Mechanics a-Solids* 35 (2012) 119–127.
- [37] M. Sauter, C. Wieners, On the superlinear convergence in computational elasto-plasticity, *Computer Methods in Applied Mechanics and Engineering* 200 (49-52) (2011) 3646–3658.
- [38] W. Han, B. D. Reddy, *Plasticity : mathematical theory and numerical analysis*, Springer, New York, 1999.
- [39] J. Albery, C. Carstensen, D. Zarrabi, Adaptive numerical analysis in primal elastoplasticity with hardening, *Computer Methods in Applied Mechanics and Engineering* 171 (34) (1999) 175–204.
- [40] P. G. Gruber, J. Valdman, Solution of one-time-step problems in elastoplasticity by a slant newton method, *SIAM Journal on Scientific Computing* 31 (2) (2009) 1558–1580.